SVD-based Scattered Small Targets Detection

Jingli Gao
College of Electrical Engineering
Zhejiang University
Hangzhou 310027, China
Email: gjl991@163.com

Chenglin Wen*
College of Electrical Engineering
Henan University of Technology
Zhengzhou 450001, China
Email: wencl@hdu.edu.cn

Meiqin Liu
College of Electrical Engineering
Zhejiang University
Hangzhou 310027, China
Email: liumeiqin@zju.edu.cn

***Abstract*—Due to lack of sufficient shape and strength information about the targets present in the entire image obtained in a wide range of scenarios over a long distance, it is very hard to detect these targets using the existing detection methods. In order to solve this problem, this paper proposes a scattered small target detection algorithm based on singular value decomposition. First, the detectability of a single target is analyzed from the perspective of singular values; second, the detectability of scattered targets is analyzed in terms of singular values and elementary transformations, based on the composability of dispersed targets, the dispersed targets can be combined into a large target using elementary transformations, on this basis, the conclusion is given that the image containing dispersed targets and the image containing a large target have the same detectability; then perform singular value decomposition on the image that may contain dispersed targets and the standard residual image which does not contain targets, and obtain their respective singular value vectors, use these singular value vectors to calculate the cosine angle which was used to determine whether the image contains targets or not, if it is confirmed, the targets are roughly located based on the singular vectors. Finally, the effectiveness of the algorithm is verified using Monte Carlo simulation.**

I. Introduction

Due to limitations of imaging hardware equipment and imaging environment, the potential targets obtained in a wide range of scenarios over a long distance show some drawbacks such as insufficient shape and intensity information, the conventional detection methods can not detect the existence of such targets. However, such missed targets can cause serious security threat in steel, aviation and other areas [1]-[8].

For small target detection problem, there are methods based on wavelet transform (WT) [4], mathematical morphology (MM) [5] and singular value decomposition (SVD) [6]-[8]. The method based on wavelet transform applies multiscale decomposition on the image that may contain a target, abandons the low-frequency wavelet coefficients, and performs threshold denoising and enhancement on the high frequency wavelet coefficients, then reconstructs the image and finally completes the target detection using threshold segmentation [4]. Wavelet based method makes good use of multiscale characteristics of the target, but when the target is very weak, it is difficult to obtain its multiscale description. Method based on mathematical morphology uses Top-hat transform to obtain the target image without of background, enhances the target contrast using sharpening operator, and then applies threshold segmentation to complete the target detection [5]. Method based on mathematical morphology makes good use of morphological information of the target, but when the shape information of the small target is insufficient, the detection performance is poor. SVD-based method in [6] uses the mean of the singular values of all sub-images as a threshold, and performs threshold segmentation by comparing the threshold with the mean of singular values of each sub-image to complete target detection. SVD-based method in [7] uses the squares of the largest singular values of sub-images as the characteristics for cluster segmentation to complete target detection. The detection performance of methods in [6]-[7] is related to the selection of block size and threshold, which are difficult to select when the size and intensity information about the target are insufficient. Both the two SVD-based methods use the local singular value features, but did not consider the relationship between the adjacent singular values. The algorithm in [8] uses the global singular value features to constitute singular value vectors, and complete the target detection using the cosine angle of singular value vectors reflecting the relationship between the neighboring singular values. The detection methods described above, generally require that the target has sufficient shape and intensity information and so on, so the target is difficult to detect when lack of sufficient information.

In order to solve the detection problem which is very difficult when lack of shape and intensity information about the target, this paper proposes a detection algorithm for dispersed targets based on elementary transformation and SVD. SVD is an important algebra feature extraction method, the singular values of image have the characteristics of stability, scale invariance, transposition invariance, rotating invariance, shift invariance and mirror invariance[9]-[10], and the singular vectors of image have the advantage of positioning targets[8]. For the image containing dispersed targets, the accumulation of dispersed targets in intensity or size will make the increments of singular values uneven, and for image containing no targets, its singular values can produce only small disturbance according to the stability of the singular values. Therefore, when the cumulative information about intensity or size of dispersed targets in an image is up to a certain extent, its singular values can be used as features to distinguish itself from the image which does not contain targets. Here the cosine angle of singular value vectors consisting of singular values is used as a criterion to determine whether the image to be detected contains targets or not.

Section II discusses the detectability of a single target from the perspective of the intensity and size change of the target.

This work was supported by the National Nature Science Foundation of China (61273170, 61304109, 61174142, 61203094)

*Corresponding Author

Section III discusses the detectability of dispersed targets, proves that the image containing dispersed targets and the image containing combined target are with the same detectability, on this basis, the cosine angle is used to complete the detection of scattered targets. Section IV performs Monte Carlo simulation to demonstrate the effectiveness of the proposed algorithm. Section V is a summary and discussion.

II. Detectability of Single Target

This section discusses the detectability of a single target in an image. The images occurred in the following paper refer to the images without of background. Assuming that the intensity of the target remains unchanged, discuss the impact of its size changes on the singular values of the image; assuming that the size of the target remain unchanged, discuss the impact of its intensity changes on the singular values of the image.

Definition 2.1[11] Denote the residual image wiping off background by $X_k \in R^{m\times n}$, the element of X_k is such that

$$X_k(i,j) = \begin{cases} d_{ij} + \epsilon_{ij}, & (i,j) \in C \\ \epsilon_{ij}, & (i,j) \notin C \end{cases} \tag{1}$$

where ϵ_{ij} is independent and identically distributed standard Gaussian random variable, d_{ij} can be any real number which denotes the intensity of a possible target, C is subset of X_k and denotes the target area.

Definition 2.2[10],[13]For a general matrix, denoting $X_0 \in R^{m\times n}$, $rank(X_0) = r_0$, then there exists a m-order unitary matrix U_0 and, a n-order unitary matrix V_0, such that

$$X_0 = U_0 S_0 V_0^T = U_{0r_0} S_{0r_0} V_{0r_0}^T \tag{2}$$

where $S_0 = \begin{bmatrix} S_{0r_0} & 0 \\ 0 & 0 \end{bmatrix}$, $S_{0r_0} = diag[s_{01}, s_{02}, \cdots, s_{0r_0}]$, $U_0 = [U_{0r_0}, U_{0(m-r_0)}] \in R^{m\times m}$, $U_{0r_0} = [u_{01}, u_{02}, \cdots, u_{0r_0}]$, $U_{0(m-r_0)} = [u_{0(r_0+1)}, \cdots, u_{0m}]$, $V_0 = [V_{0r_0}, V_{0(n-r_0)}] \in R^{n\times n}$, $V_{0r_0} = [v_{01}, v_{02}, \cdots, v_{0r_0}]$, $V_{0(n-r_0)} = [v_{0(r_0+1)}, \cdots, v_{0n}]$.

Equation (2) is called singular value decomposition of the matrix X_0, $\{s_i\}_{i=1}^{r_0}$ are the nonzero singular values of X_0, and the column vectors of U_0 and V_0 are referred to as the left and right singular vectors respectively.

Definition 2.3[13] Let $X = X_0 + \epsilon X_t$, $0 < |\epsilon| < 1$, $X_t \in R^{m\times n}$, then the singular value decomposition of X is

$$X = USV^T = U_r S_r V_r^T \tag{3}$$

where $rank(X) = r$, the meanings of the symbols in the formula (3) can be obtained by the corresponding symbols in the formula (2) after removing the subscript 0.

Theorem 2.1 Let $X = X_0 + \epsilon X_t$, X_0 denotes the image to be detected which conforms to Definition 2.1, and has no multiple nonzero singular values, namely $s_{01} > s_{02} > \cdots > s_{0r_0} > s_{0(r_0+1)} = s_{0(r_0+2)} = \cdots = s_{0n}$; X_t denotes the image whose pixel values are zero except for the pixels of the target in it, suppose that the pixels of the target have the same value d for simplicity, namely $X_t(g,h) = d, g = g_1, g_2, \cdots, g_w, h = h_1, h_2, \cdots, h_z$; according to Definition 2.3 and the convergent power series about ϵ [13], for $\epsilon = 1$, the power series approximating the singular values of X can be written as

$$s_i = s_{0i} + A_i + \frac{1}{2}B_i \tag{4}$$

where $1 \le i \le p \le r_0$, and

$$\begin{aligned}
A_i &= d \sum_{g=g_1}^{g_w} u_{0i}(g) \sum_{h=h_1}^{h_z} v_{0i}(h), \\
B_i &= C_i + D_i + E_i + F_i + G_i, \\
F_i &= \sum_{j=r_0+1}^{n} \frac{d^2}{s_{0i}} (\sum_{g=g_1}^{g_w} u_{0i}(g) \sum_{h=h_1}^{h_z} v_{0j}(h))^2, \\
G_i &= \sum_{j=r_0+1}^{m} \frac{d^2}{s_{0i}} (\sum_{g=g_1}^{g_w} u_{0j}(g) \sum_{h=h_1}^{h_z} v_{0i}(h))^2, \\
C_i &= (\sum_{g=g_1}^{g_w} u_{0i}(g) \sum_{h=h_1}^{h_z} v_{0i}(h)) \sum_{j=1}^{r_0} \frac{2d^2 s_{0j}}{s_{0i}^2 - s_{0j}^2} \\
&(\sum_{g=g_1}^{g_w} u_{0j}(g) \sum_{h=h_1}^{h_z} v_{0j}(h)), \\
D_i &= \sum_{j=1}^{r_0} \frac{2d^2 s_{0j}}{s_{0i}^2 - s_{0j}^2} (\sum_{g=g_1}^{g_w} u_{0i}(g) \sum_{h=h_1}^{h_z} v_{0j}(h))^2, \\
E_i &= \sum_{j=1}^{r_0} \frac{2d^2 s_{0j}}{s_{0i}^2 - s_{0j}^2} (\sum_{g=g_1}^{g_w} u_{0j}(g) \sum_{h=h_1}^{h_z} v_{0i}(h))^2.
\end{aligned} \tag{5}$$

In the formula (5), B_i consists of five parts. A_i denotes the projection of X_t onto pattern $u_{0i}v_{0i}^T$. F_i represents the weighted sum squares of projections of X_t onto patterns $u_{0i}v_{0(r_0+1)}^T, \cdots, u_{0i}v_{0n}^T$, G_i represents the weighted sum squares of projections of X_t onto patterns $u_{0(r_0+1)}v_{0i}^T, \cdots, u_{0m}v_{0i}^T$, F_i and G_i can be neglected, because singular vectors $v_{0(r_0+1)}, \cdots, v_{0n}$ and $u_{0(r_0+1)}, \cdots, u_{0m}$ correspond to zero singular values and contain no useful information. For $i > 1$, C_i represents the difference between the weighted sum squares of projections of X_t onto patterns $u_{0(i+1)}v_{0(i+1)}^T, \cdots, u_{0r_0}v_{0r_0}^T$ and the weighted sum squares of projections of X_t onto patterns $u_{0(i-1)}v_{0(i-1)}^T, \cdots, u_{01}v_{01}^T$; D_i represents the difference between the weighted sum squares of projections of X_t onto patterns $u_{0i}v_{0(i+1)}^T, \cdots, u_{0i}v_{0r_0}^T$ and the weighted sum squares of projections of X_t onto patterns $u_{0i}v_{0(i-1)}^T, \cdots, u_{0i}v_{01}^T$; E_i represents the difference between the weighted sum squares of projections of X_t onto patterns $u_{0(i+1)}v_{0i}^T, \cdots, u_{0r_0}v_{0i}^T$ and the weighted sum squares of projections of X_t onto patterns $u_{0(i-1)}v_{0i}^T, \cdots, u_{01}v_{0i}^T$. With the increase of index i, the absolute value of C_i, D_i, E_i will gradually decrease. For $i = 1$, C_i represents the weighted sum squares of projections of X_t onto patterns $u_{02}v_{02}^T, \cdots, u_{0r_0}v_{0r_0}^T$; D_i represents the weighted sum squares of projections of X_t onto patterns $u_{01}v_{02}^T, \cdots, u_{01}v_{0r_0}^T$; E_i represents the weighted sum squares of projections of X_t onto patterns $u_{02}v_{01}^T, \cdots, u_{0r_0}v_{01}^T$. From the above analysis, it can be concluded that the increase of different singular values may be uneven, the increment depends on the singular values and singular vectors containing pattern information.

The target detectability refers to the required minimum intensity and size of the target when it can be detected. The intensity of the target in an image refers to the gray value of the target, and the size of the target in an image refers to the number of pixels of the target[12]. From the view of accumulation in intensity or size, the target detectability is analyzed as follows.

Case 1, assuming the intensity of the target remains unchanged, increase the size of the target. Assuming the size of the target in the image X_0 is very small, the target can not be effectively identified. As is shown in Fig.1(a), the size of the target is increased, the increase portion of the target is denoted by Δ_C, and this increment will cause the changing of A_i and B_i, which affect the change of the singular values of X. Since the intensity of the target remains unchanged, thus for different increment of target size Δ_C, the effective area of projection is partially changed. Fig.1(a) shows that the projection range of Δ_C onto u_i is changed to $[g_1, g_2, \cdots, g_w]$; the projection range of Δ_C onto v_i is unchanged, and is still $[h_1, h_2, \cdots, h_z]$. Therefore, the change of singular values mainly depends on the patterns contained in sub-images of X_0. Let $\Delta_i = A_i + \frac{1}{2}B_i$, when all the values of Δ_i are relatively close, it shows that the energy cumulated by the increment of the target size is insufficient to determine the existence of the target itself, and the large difference of the values Δ_i indicates that the target in the image X exists.

Case 2, assuming the size of the target remains unchanged, increase the intensity of the target. Assuming the intensity of the target in the image X_0 is very low, the target can not be effectively detected. Fig.1(b) shows that, the intensity of the target is increased, the increase part of the target is expressed as Δ_C, and this increment will also cause the changing of A_i and B_i, which determine the change of the singular values of X. Since the size of the target remains unchanged, thus for different increment of target intensity, the effective area of projection is unchanged. As is shown in Fig.1(b), the projection range of Δ_C onto u_i is still $[g_1, g_2, \cdots, g_w]$; the projection range of Δ_C onto v_i is still $[h_1, h_2, \cdots, h_z]$. Therefore, the change of singular values mainly depends on intensity information. Let $\Delta_i = A_i + \frac{1}{2}B_i$, when the values of Δ_i are relatively close, it shows that the energy cumulated by the increment of the target intensity is insufficient to determine the existence of the target itself, and the large difference of the values Δ_i indicates that the existence of the target in the image X is true.

According to the above discussion, in either case, the energy accumulated from changes of intensity or size of the target will result in the change of the singular values of X. When such non-uniform changes of the singular values is up to a certain extent, an angle will occur between the vector composed of these singular values and the singular value vector of the standard residual image containing no target, so the angle can be used to express this uneven change of singular values.

III. Detectability of Scattered Targets

This section discusses the detectability of dispersed targets. If several small targets can be effectively transformed into a big target through elementary transformations, then the image containing a number of small targets and the image containing a big target have consistent detectability.

Definition 3.1[14] Let $I \in R^{n\times n}$ denote the identity matrix. Apply the elementary row or column transformation to the identity matrix, and obtain

$$P(i,j) = E_{ij} + E_{ji} + \sum_{k\neq i,j} E_{kk} \tag{6}$$

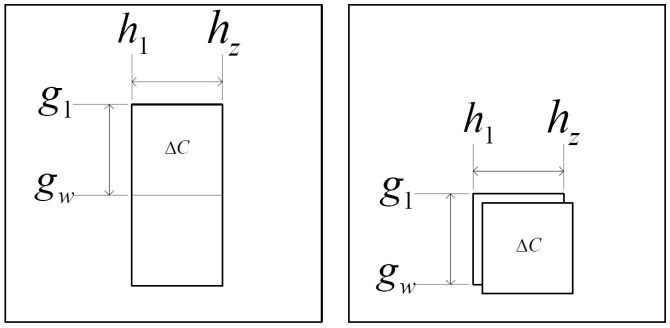

Fig. 1. Sketch of size or intensity accumulation of the target in an image; (a)assuming the intensity of the target remains unchanged, increase the size of the target(left), (b)assuming the size of the target remains unchanged, increase the intensity of the target(right).

where $E_{ii} = E_{jj} = 0, E_{kk} = 1(k \neq i,j)$; the off-diagonal elements $E_{ij} = E_{ji} = 1$, and the remainders are zero.

Theorem 3.1 Assuming $X \in R^{m\times n}$, exchange the ith row and the jth row or exchange the ith column and the jth column, then the form of singular value decomposition of X remains unchanged.

Proof: By Definition 3.1, apply the elementary row transformation to the matrix X, and obtain matrix $B = P(i,j)X$, where $P(i,j) = E_{ij} + E_{ji} + \sum_{k\neq i,j} E_{kk}$. In terms of $P(i,j)P(i,j)^T = P(i,j)^T P(i,j)$, it is known that the matrix $P(i,j)$ is unitary. Apply singular value decomposition to the matrix X, and denote $X = USV^T$. By definition 2.3, it is known that the matrix U is unitary, so $P(i,j)U$ is unitary [10]. Therefore, the singular value decomposition of the matrix B can be written as

$$B = P(i,j)X = P(i,j)USV^T = (P(i,j)U)SV^T \tag{7}$$

Similarly, perform the elementary column transformation on the matrix X, and obtain the singular value decomposition of the matrix B as

$$B = XP(i,j) = USV^T P(i,j) = US(V^T P(i,j)) \tag{8}$$

Therefore, by the definition of singular value decomposition, exchange the ith row and the jth row or exchange the ith column and the jth column, the form of singular value decomposition of X remains unchanged. ■

Definition 3.2 If the dispersed targets in an image can be combined into a single large target by elementary transformations, then this feature is called composability of the scattered targets; similarly, if the large target in an image can be divided into scattered targets by elementary transformations, then this feature is called decomposability of the large target.

Typically, due to the intensity or size information of a small target is very weak and it is difficult to detect such target, but a large target combined from dispersed targets is easier to detect. This is the detectability of scattered targets. According to Definition 3.2 and Theorem 3.1, it is shown that if the scattered targets in the image X satisfies composability, then the image X containing the scattered targets can be transformed into the image B containing the big target through several elementary transformations, and the image

X and the image B have the same form of singular value decomposition, namely, $B = (PU)S(V^TQ)$, where P is the product of several elementary matrices corresponding to the elementary row transformations, and Q is the product of several elementary matrices corresponding to the elementary column transformations. Therefore, the image containing small targets and the image containing a big target have the same singular value vector, in other words, the detectability of the image X and the image B is consistent in the sense of elementary transformations.

In fact, as long as the dispersed targets meet the linear arrangement, in other words, these targets are placed in straight rows or columns, or any two of these targets have no same row and column numbers, then these dispersed targets can be effectively combined by elementary transformations. The primary cause of detectability of the image containing scattered targets is the energy accumulation of the targets on their arrangement direction, and in all directions, the energy accumulated along the arrangement direction is maximum.

From the above discussion, based on the rule of cosine angle of singular value vectors, the detection algorithm for dispersed targets is given as follows.

- Obtain the image X_k containing composible dispersed targets.
- Calculate the singular value vector of X_k and the singular value vector of the standard residual image containing no targets, and use these vectors to compute the cosine angle which is used to determine whether the image X_k contains targets, where each element of the standard residual image is independent and identically distributed standard Gaussian random variable.
- If the image contains targets, then the rough location of the dispersed targets is given according to its singular vectors.

IV. Experimental Results

A. Experiment for Detectability of Targets

Experiment 1, assuming that the average intensity of the target in an image remains unchanged, test to see how large the size of the target is when it can be detected. Assuming that the average intensity of the target is d, the pixel values of target is located in $[d-1, d+1]$. The sliding interval of d is $[1, 29]$. For each value of d, let the size of the target increase from 1×1, until the size is large enough for the target to be detected. TABLE I shows the results of four methods: singular value vector angle (CA [8]), the wavelet transform (WT [4]), mathematical morphology (MM [5]) and sub-block image singular value Mean (MS [6]). The first column of TABLE I shows the intensity range and the average intensity of the target, the second, third, fourth and fifth columns give the size of the target when it can be detected using CA, WT, MM and MS methods respectively. The symbol '$\times$' in TABLE I indicates misjudgement, i.e., the detection size is incorrect. As can be seen from TABLE I, when the mean intensity of the target is small, due to the impact of noise, WT, MM and MS methods are likely to cause miscarriage of justice, although CA method requires a larger size for the target to be detected, compared to other methods, it is still valid. When the average intensity of the target is less than 9, CA method requires a size larger than the other three methods for it to be detected, as the other three methods rely on the local characteristics; When the average intensity of the target is greater than 9, CA method requires a size slightly larger than WT and MS methods, while slightly less than MM method for it to be detected. Generally speaking, WT, MM and MS methods rely on local features, when the average intensity of the target is greater than a certain value, the size of the target has little influence on its detectability.

TABLE I. RELATIONSHIP BETWEEN DETECTABILITY AND SIZE WHEN THE INTENSITY IS FIXED

[d-1,d+1]d	detectable size			
	CA [8]	WT [4]	MM [5]	MS [6]
[0,2]1	27*27	×	×	×
[1,3]2	13*13	×	×	×
[2,4]3	8*8	3*3	3*3	5*5
[3,5]4	7*7	3*3	3*3	×
[4,6]5	5*5	3*3	3*3	2*2
[5,7]6	5*5	3*3	3*3	2*2
[6,8]7	4*4	3*3	3*3	2*2
[7,9]8	4*4	2*2	3*3	2*2
[8,10]9	3*3	2*2	3*3	1*1
[9,11]10	3*3	1*1	3*3	1*1
[10,12]11	3*3	3*3	3*3	2*2
[11,13]12	2*2	1*1	3*3	1*1
[12,14]13	3*3	1*1	3*3	1*1
[13,15]14	2*2	1*1	3*3	1*1
[14,16]15	2*2	1*1	3*3	1*1
[15,17]16	2*2	1*1	3*3	1*1
[16,18]17	2*2	1*1	3*3	1*1
[17,19]18	2*2	1*1	3*3	1*1
[18,20]19	2*2	1*1	3*3	1*1
[19,21]20	2*2	1*1	3*3	1*1
[20,22]21	2*2	2*2	3*3	2*2
[21,23]22	2*2	1*1	3*3	1*1
[22,24]23	1*1	2*2	3*3	1*1
[23,25]24	2*2	1*1	3*3	1*1
[24,26]25	2*2	1*1	3*3	1*1
[25,27]26	1*1	1*1	3*3	1*1
[26,28]27	1*1	2*2	3*3	1*1
[27,29]28	1*1	1*1	3*3	1*1
[28,30]29	1*1	1*1	3*3	2*2

Experiment 2, assuming that the size of the target remains unchanged, test to see how large the intensity of the target is when it can be detected. Assuming that the size of the target is $N \times N$, $N \in [1, 29]$. For each size $N \times N$, let the average intensity d of the target increase from 1, until the intensity is large enough for the target to be detected, the sliding interval of d is $[d-1, d+1]$. TABLE II shows the results of CA, WT, MM and MS methods. The first column of TABLE II shows the size of the target, the second, third, fourth and fifth columns give the sliding interval $[d-1, d+1]$ and average intensity d of the target for it to be detected using CA, WT, MM and MS methods respectively. The symbol '$\times$' in TABLE II indicates misjudgment, i.e., the detection intensity is incorrect. As can be seen from Table II, when the size of the target is less than 10*10, CA method requires an average intensity larger than the other three methods for it to be detected; when the size of the target is greater than 10*10, CA method requires an average intensity slightly less than WT and MM methods, and almost the same as MS method. Generally speaking, WT, MM and MS methods rely on local features, therefore, the impact of target size on these three methods is less than CA method.

From analysis of the experiment 1 and the experiment 2,

TABLE II. RELATIONSHIP BETWEEN DETECTABILITY AND INTENSITY WHEN THE SIZE IS FIXED

N*N	detectable average intensity			
	CA [8]	WT [4]	MM [5]	MS [6]
1*1	[22,24]23.71	[8,10]8.85	×	[6,8]7.55
2*2	[13,15]13.87	[7,9]7.93	×	×
3*3	[7,9]8.35	[3,5]3.98	[3,5]3.98	[3,5]3.98
4*4	[6,8]7.06	[3,5]4.08	[2,4]2.83	[2,4]2.83
5*5	[4,6]4.91	[3,5]4.12	[1,3]1.93	[1,3]1.93
6*6	[4,6]4.92	[3,5]4.06	[2.4]3.02	[1,3]1.91
7*7	[3,5]4.17	[2,4]3.05	[1,3]2.08	[0,2]1.07
8*8	[3,5]3.97	[3,5]3.97	[2,4]2.94	[1,3]1.94
9*9	[3,5]4.07	[2,4]2.95	[2,4]2.95	[1,3]1.98
10*10	[2,4]2.96	[2,4]2.96	[2,4]2.96	[0,2]0.95
11*11	[2,4]2.99	[2,4]2.99	[1,3]2.02	×
12*12	[1,3]2.06	[3,5]4.02	[2,4]2.95	[1,3]2.06
13*13	[1,3]1.98	[2,4]3.06	[2,4]3.06	[0,2]1.06
14*14	[1,3]1.99	[2,4]2.96	[2,4]2.96	[0,2]0.97
15*15	[1,3]2.00	[1,3]2.00	[3,5]3.91	[1,3]2.00
16*16	[1,3]2.00	[2,4]3.01	[3,5]3.99	[1,3]2.00
17*17	[1,3]1.97	[2,4]3.06	×	[1,3]1.97
18*18	[1,3]2.02	[1,3]2.02	[3,5]4.02	×
19*19	[1,3]1.99	[3,5]3.95	[2,4]3.00	[1,3]1.99
20*20	[1,3]1.98	[2,4]2.98	[3,5]3.98	[1,3]1.98
21*21	[1,3]2.00	[1,3]2.00	[3,5]4.04	[1,3]2.00
22*22	[1,3]1.99	[3,5]3.99	[3,5]3.99	[0,2]0.98
23*23	[1,3]1.98	[1,3]1.98	[0,2]1.00	[1,3]1.98
24*24	[0,2]1.03	[3,5]3.97	[3,5]3.97	[2,4]2.99
25*25	[0,2]1.01	[2,4]2.98	[3,5]3.96	[1,3]2.00
26*26	[0,2]1.04	[3,5]3.99	[3,5]3.99	[3,5]3.99
27*27	[0,2]1.00	[2,4]3.00	[3,5]3.98	[1,3]2.00
28*28	[0,2]1.01	[3,5]3.99	[4,6]5.00	[1,3]2.03
29*29	[0,2]0.99	[1,3]2.00	[5,7]5.99	[1,3]2.00

TABLE III. RELATIONSHIP BETWEEN DETECTABILITY AND INTENSITY, NUMBER OF SCATTERED TARGETS

$[d_1, d_2]$	$count$	min	max
[0,1]	41(×)	0.3	0.6
[0,2]	32(√)	0.7	1.3
[0,3]	17(√)	0.9	1.9
[0,4]	10(√)	1.6	2.2
[0,5]	7(√)	1.9	3.0
[1,2]	17(√)	1.4	1.6
[1,3]	11(√)	1.7	2.2
[1,4]	7(√)	2.1	2.8
[1,5]	5(√)	2.8	3.5
[2,3]	7(√)	2.3	2.6
[2,4]	5(√)	2.9	3.1
[2,5]	3(√)	3.4	3.8
[3,4]	3(√)	3.5	3.6
[3,5]	3(√)	3.9	4.3
[4,5]	3(√)	4.5	4.6

it is shown that WT, MM and MS methods can successfully detect the target with a certain size and intensity, but for the target with smaller size and intensity, the detection performance is poor; CA method can decrease the intensity with the increase of target size for the target to be detected, and therefore this method provides a feasible way for scattered small target detection.

TABLE I and TABLE II here are the Monte Carlo simulation results randomly selected.

B. Experiments for Scattered Target Detection

Assuming that the image containing scattered targets has been obtained, and has the size of 256×256, each of the targets has the size of 4×4. Let the leftmost column of the first scattered target overlap with the $10th$ column of the image, and the interval between two adjacent targets is two pixels, so there are at most 41 dispersed targets in the image in the sense of elementary transformation. Let the intensity of each target be in the interval $[d_1, d_2]$, where $d_1 = 0, \cdots, 4, d_2 = 1, \cdots, 5, d_1 < d_2$, so there are 15 kinds of combinations for d_1 and d_2. The detection algorithm in section III is validated using these 15 kinds of cases. TABLE III describes the detection result randomly selected. The first column of TABLE III shows the interval of the intensity of the scattered target; the second column of TABLE III gives the number $count$ of scattered targets when they can be detected, the symbol '$\times$' indicates the detection is successful, the symbol '$\surd$' indicates the detection fails; the third and fourth columns of TABLE III show the minimum average intensity min and maximum average intensity max of scattered targets respectively, when they can be detected. As can be seen from the first row of TABLE III, when the intensity of the target varies between $[0, 1]$, the targets can not be detected due to the low signal-to-noise ratio. In Fig.2, the images of the first column correspond to the 15 kinds of cases shown in TABLE III, the figures of the second and third columns represent their first left and right singular vectors respectively. As can be seen from Fig.2, except for the first row indicating the detection fails, the remaining 14 rows indicate that the detection is successful, and the rough position can be indicated by the first left singular vectors and right singular vectors.

V. CONCLUSION

This paper presents a scattered small target detection algorithm based on SVD and elementary transformation. As long as the dispersed targets can be combined into a large target through elementary transformations, the existence of targets in the image can be determined through the accumulation of energy. In this paper, only the composable targets are discussed. However, for the targets which do not satisfy the composable condition, their detection problem should be reserved for further consideration. Meanwhile this paper assumes that the image containing dispersed targets has already been acquired, in fact, the search algorithms or other methods are required to obtain the image containing scattered targets. So, how to get the image containing scattered targets will be the next work to be considered.

REFERENCES

[1] W. Zhang, M. Y. Cong, L. P. Wang, "Algorithm for optical weak small targets detection and tracking: Review," in *Proc. IEEE 2003 International Conference on Neural Networks and Signal Processing*, Nanjing, China, Dec. 2003, vol. 1, pp. 643-647.

[2] M. Yazdchi, M. Yazdi, A. G. Mahyari, "Steel Surface Defect Detection Using Texture Segmentation Based on Multifractal Dimension," in *Proc. 2009 International Conference on Digital Image Processing*, Bangkok, Thailand, March. 2009, pp. 346-350.

[3] X. H. Xie, "A review of recent advances in surface defect detection using texture analysis techniques," *Electronic Letters on Computer Vision and Image Analysis*, vol. 7, no. 3, pp. 1-22, 2008.

[4] L. Cheng, "Wavelet analysis based infrared dim small target detection algorithm," *Journal of Anyang Institute of Technology*, no. 4, pp. 41-43, 2008.

[5] C. J. Zang, G. X. Li,Y. .X. Wang, "Infrared dim target detection using morphology based method," *Journal of Air Force Radar Academy*, vol. 26, no. 2, pp. 94-97, 2012.

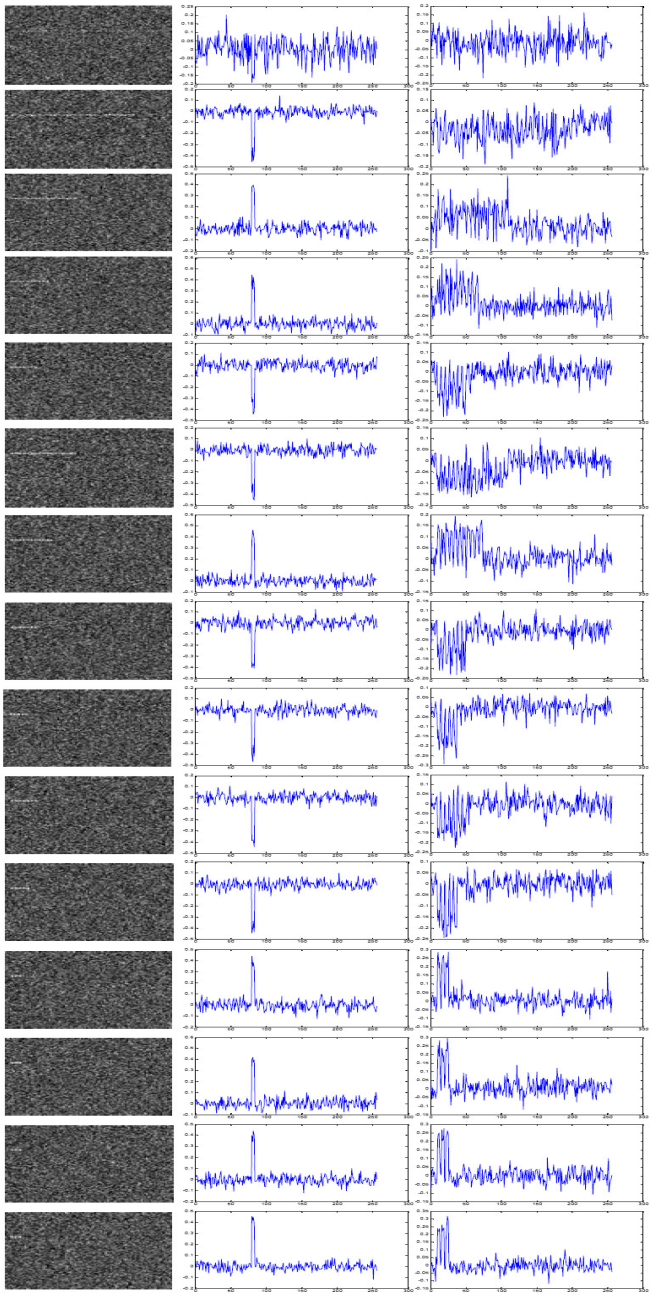

Fig. 2. Images and singular vectors; the images corresponding to 15 combinations(left), their first left singular vectors(center), their first right singular vectors(right)

[6] S. .Y. Chen, J. Feng, "Research on detection of fabric defects based on singular value decomposition," in *Proc. 2010 IEEE International Conference on Information and Automation*, Harbin, China, June. 2010, pp. 857-860.

[7] L. Tomczak, V. Mosorov, "Singular value decomposition for texture defect detection in visual inspection systems," in *Proc. the 2nd International Conference on Perspective Technologies and Methods in MEMS Design*, Lviv-Polyana, UKRAINE, May. 2006, pp. 131-133.

[8] J. L. Gao, C. L. Wen, M. Q.Liu, "Steel surface defect detection and localization based on SVD and two-side compressive measurements," in *Proc. the 26th Chinese Control and Decision Conference*, Changsha, China, May-June. 2014, pp. 1401-1406.

[9] Z. Q. Hong, J. Y. Yang, "Algebraic feature extraction of image for recognition," *Acta automatica sinica*, vol. 18, no. 2, pp. 233-237, 1992.

[10] R. C. Shi, F. Wei, *Matrix Analysis*, Beijing institute of technology press, 2005.

[11] H. Y. Li, C. K. Wu, "A new algorithm for detecting and tracking dim point-source target in image sequences," *Journal of Xidian University*, vol. 27, no. 3, pp. 317-321, 2000.

[12] H. Zhang. "Researches on UAV based moving targets detection and tracking and vision aided UAV landing system," Doctor's thesis, National university of defense technology, Changsha, 2008.

[13] Z. H. Lv, "Direct perturbation method for reanalysis of matrix singular value decomposition," *Applied mathematics and mechanics*, vol. 18, no. 5, pp. 441-446, 1997.

[14] D. J. meng, *Higher algebra and analytic geometry*, Science press, 2007.